Fluid Turbulence in Quantum Plasmas

Dastgeer Shaikh*
Institute of Geophysics and Planetary Physics, University of California, Riverside, CA 92521

P. K. Shukla†
Institut für Theoretische Physik IV, Ruhr-Universität Bochum, D-44780 Bochum, Germany, and School of Physics, University of KwaZulu-Durban, Durban 4000, South Africa

(Received 19 February 2007; Revised 30 May 2007)

Nonlinear fluid simulations are carried out to investigate the properties of fully developed two-dimensional (2D) electron fluid turbulence in a dense Fermi (quantum) plasma. We report several distinguished features that have resulted from our 2D computer simulations of the nonlinear equations which govern the dynamics of nonlinearly interacting electron plasma oscillations (EPOs) in the Fermi plasma. We find that a 2D quantum electron plasma exhibits dual cascades, in which the electron number density cascades towards smaller turbulent scales, while the electrostatic potential forms larger scale eddies. The characteristic turbulent spectrum associated with the nonlinear electron plasma oscillations exhibits a non-Kolmogorov-like feature in a weak quantum tunneling regime, and it tends to relax towards a $k^{-3/2}$ spectrum, where k is the wave-number. By contrast, the turbulent spectrum condensates toward smaller modes when tunneling effects are strong. Consequently, the turbulent transport corresponding to the large-scale structures is predominant in comparison with the small-scales associated with electron number density variations, a result that is consistent with the classical diffusion theory.

PACS numbers: 52.27.Gr,52.35.Ra,71.10Ca

About forty five years ago, Pines [1] had laid down foundations for quantum plasma physics. During the last decade, there has been a growing interest in investigating new aspects of dense quantum plasmas by developing the quantum hydrodynamic (QHD) equations [2] by incorporating the quantum force associated with the Bohm potential [2], by deriving the Child-Langmuir law in the quantum regime [3], and by studying numerous collective effects [4–7] involving different quantum forces (e.g. due to the Bohm potential [2] and the pressure law [4, 5] for the Fermi plasma, as well as the potential energy of the electron−1/2 spin magnetic moment in a magnetic field [9]). Studies of collective interactions in dense quantum plasmas are relevant for the next generation intense laser-solid density plasma experiments [10, 11], for superdense astrophysical bodies [12, 13] (e.g. the interior of white dwarfs and neutron stars), as well as for micro and nano-scale objects (e.g. quantum diodes [3], quantum dots and nanowires [14], nano-photonics [15]).

The the Wigner-Poisson (WP) model [16] has been used to derive a set of quantum hydrodynamic (QHD) equations [4, 5] for a dense electron plasma. The QHD equations include the continuity, momentum and Poisson equations. The quantum nature [4] appears in the electron momentum equation through the pressure term, which requires the knowledge of the Wigner distribution for a quantum mixture of electron wave functions, each characterized by an occupation probability. The quantum part of the electron pressure is represented as a quantum force [2, 4] $-\nabla\phi_B$, where $\phi_B = -(\hbar^2/2m_e\sqrt{n_e})\nabla^2\sqrt{n_e}$, $\hbar$ is the Planck constant divided by 2π, m_e is the electron mass, and n_e is the electron number density. Defining the effective wave function $\psi = \sqrt{n_e(\mathbf{r},t)}\exp[iS(\mathbf{r},t)/\hbar]$, where $\nabla S(\mathbf{r},t) = m_e\mathbf{u}_e(\mathbf{r},t)$ and $\mathbf{u}_e(\mathbf{r},t)$ is the electron velocity, the electron momentum equation can be represented as an effective nonlinear Schrödinger (NLS) equation [4, 5, 7], in which there appears a coupling between the wave function and the electrostatic potential associated with the EPOs. The electrostatic potential is determined from the Poisson equation. We thus have the coupled NLS and Poisson equations, which govern the dynamics of nonlinearly interacting EPOs is a dense quantum plasmas. This mean-field model of Ref. [4, 5] is valid to the lowest order in the correlation parameter, and it neglects correlations between electrons. The density functional theory [8] incorporates electron-electron correlations, which are neglected in the present paper.

In this Letter, we use the coupled NLS and Poisson equations for investigating, by means of computer simulations, the properties of 2D electron fluid turbulence and associated electron transport in quantum plasmas. We find that quantum tunneling effects play a crucial role in the evolutionary processes. For instance, the nonlinear coupling between the EPOs of different scale sizes gives rise to small-scale electron density structures that co-exist with large scale electrostatic potential structures in a weak quantum tunneling regime. Furthermore, the total energy associated with quantum electron plasma exhibits a *non-* Kolmogorov-like turbulent spectrum. On the other hand, strong quantum tunneling yields a char-

*Electronic address: dastgeer@ucr.edu
†Electronic address: ps@tp4.rub.de

acteristic turbulent spectrum that condensates at the smaller modes resulting in the large scale structures in both electron density and electrostatic potential. The electron diffusion caused by the electron fluid turbulence is consistent with the dynamical evolution of turbulent mode structures.

For our 2D turbulence studies, we use the nonlinear Schrödinger-Poisson equations [4, 7]

$$i\sqrt{2H}\frac{\partial \Psi}{\partial t} + H\nabla^2\Psi + \varphi\Psi - |\Psi|^2\Psi = 0, \qquad (1)$$

and

$$\nabla^2\varphi = |\Psi|^2 - 1, \qquad (2)$$

which are valid at zero electron temperature for the Fermi-Dirac equilibrium distribution, and which govern the dynamics of nonlinearly interacting EPOs of different wavelengths. In Eqs. (1) and (2) the wave function Ψ is normalized by $\sqrt{n_0}$, the electrostatic potential φ by k_BT_F/e, the time t by the electron plasma period ω_{pe}^{-1}, and the space $\mathbf{r}$ by the Fermi Debye radius λ_D. We have introduced the notations $\lambda_D = (k_BT_F/4\pi n_0e^2)^{1/2} \equiv V_F/\omega_{pe}$ and $\sqrt{H} = \hbar\omega_{pe}/\sqrt{2}k_BT_F$, where k_B is the Boltzmann constant and the Fermi electron temperature $T_F = (\hbar^2/2m_e)(3\pi^2)^{1/3}n_0^{2/3}$, e is magnitude of the electron charge, and $\omega_{pe} = (4\pi n_0e^2/m_e)^{1/2}$ is the electron plasma frequency. The origin of the various terms in Eq.(1) is obvious. The first term is due to the electron inertia, the H-term in (1) is associated from the quantum tunneling involving the Bohm potential, $\varphi\Psi$ comes from the nonlinear coupling between the scalar potential (due to the space charge electric field) and the electron wave function, and the cubic nonlinear term is the contribution of the electron pressure [4] for the Fermi plasma that has a quantum statistical equation of state.

Equations (1) and (2) admit a set of conservation laws [9], including the number of electrons $N = \int \Psi^2 dxdy$, the electron momentum $\mathbf{P} = -i\int \Psi^*\nabla\Psi dxdy$, the electron angular momentum $\mathbf{L} = -i\int \Psi^*\mathbf{r}\times\nabla\Psi dxdy$, and the total energy $\mathcal{E} = \int[-\Psi^*H\nabla^2\Psi + |\nabla\varphi|^2/2 + |\Psi|^3/2]dxdy$. In obtaining the total energy $\mathcal{E}$, we have used the relation $\partial\mathbf{E}/\partial t = iH(\Psi\nabla\Psi^* - \Psi^*\nabla\Psi)$, where the electric field $\mathbf{E} = -\nabla\varphi$. The conservations laws are used to maintain the accuracy of the numerical integration of Eqs. (1) and (2), which hold for quantum electron-ion plasmas with fixed ion background. The assumption of immobile ions is valid, since the EPOs (given by the dispersion relation [4, 5] $\omega^2 = \omega_{pe}^2 + k^2V_F^2 + \hbar^2k^4/4m_e^2$) occur on the electron plasma period, which is much shorter than the ion plasma period ω_{pi}^{-1}. Here ω and k are the frequency and the wave-number, respectively. The ion dynamics, which may become important in the nonlinear phase on a longer timescale (say of the order of ω_{pi}^{-1}), in our investigation can easily be incorporated by replacing 1 in Eq. (2) by n_i, where the normalized (by n_0) ion density n_i is determined from $d_tn_i + n_i\nabla\cdot\mathbf{u}_i = 0$ and $d_t\mathbf{u}_i = -C_s^2\nabla\varphi$, where $d_t = (\partial/\partial t) + \mathbf{u}_i\cdot\nabla$, $\mathbf{u}_i$ is the ion velocity, $C_s = (k_BT_F/m_i)^{1/2}$ is the ion sound speed, and m_i is the ion mass.

The nonlinear mode coupling interaction studies are performed to investigate the multi-scale evolution of a decaying 2D electron fluid turbulence, which is described by Eqs. (1) and (2). All the fluctuations are initialized isotropically (no mean fields are assumed) with random phases and amplitudes in Fourier space, and evolved further by the integration of Eqs. (1) and (2), using a fully de-aliased pseudospectral numerical scheme [17] based on the Fourier spectral methods. The spatial discretization in our 2D simulations uses a discrete Fourier representation of turbulent fluctuations. The numerical algorithm employed here conserves energy in terms of the dynamical fluid variables and not due to a separate energy equation written in a conservative form. The evolution variables use periodic boundary conditions. The initial isotropic turbulent spectrum was chosen close to k^{-2}, with random phases in all directions. The choice of such (or even a flatter than -2) spectrum treats the turbulent fluctuations on an equal footing and avoids any influence on the dynamical evolution that may be due to the initial spectral non-symmetry. The equations are advanced in time using a 4 th order Runge-Kutta scheme. The code is made stable by a proper de-aliasing of spurious Fourier modes, and by choosing a relatively small time step in the simulations. Our code is massively parallelized using Message Passing Interface (MPI) libraries to facilitate higher resolution in a 2D computational box of size 2π, with a resolution of 512^2 grid points.

We study the properties of 2D fluid turbulence, composed of nonlinearly interacting EPOs, for two specific physical systems. These are the dense plasmas in the next generation laser-based plasma compression (LBPC) schemes [11] as well as in superdense astrophysical objects [12, 13] (e.g. white dwarfs). It is expected that in LBPC schemes, the electron number density may reach 10^{27} cm^{-3} and beyond. Hence, we have $\omega_{pe} = 1.76\times10^{18}$ s^{-1}, $k_BT_F = 1.7\times10^{-9}$ erg, $\hbar\omega_{pe} = 1.7\times10^{-9}$ erg, and $H = 1$. The Fermi Debye length $\lambda_D = 0.1\ A^0$. On the other hand, in the interior of white dwarfs, we typically have [18] $n_0 \sim 10^{30}$ cm^{-3} (such values are also common in dense neutron stars and supernovae), yielding $\omega_{pe} = 5.64\times10^{19}$ s^{-1}, $k_BT_F = 1.7\times10^{-7}$ erg, $\hbar\omega_{pe} = 5.64\times10^{-8}$ erg, $H \approx 0.3$, and $\lambda_D = 0.025\ A^0$. The numerical solutions of Eqs. (1) and (2) for $H = 1$ and $H = 0.025$ (corresponding to $n_0 = 10^{27}$ cm^{-3} and $n_0 = 10^{30}$ cm^{-3}, respectively) are displayed respectively in top and bottom panels of Fig 1 which represent the electron number density (left) and electrostatic (ES) potential (right) distributions in the (x, y)-plane.

Of particular importance are the regimes of weak ($H \ll 1$) and strong ($H \geq 1$) quantum tunneling where the underlying model exhibits rich and complex dynamics as shown in Fig 1. Figure 1 reveals that the electron density distribution $|\Psi|^2$ (top left), in $H < 1$ regime, has a tendency to generate smaller length-scale structures, while the ES potential cascades towards larger scales (top

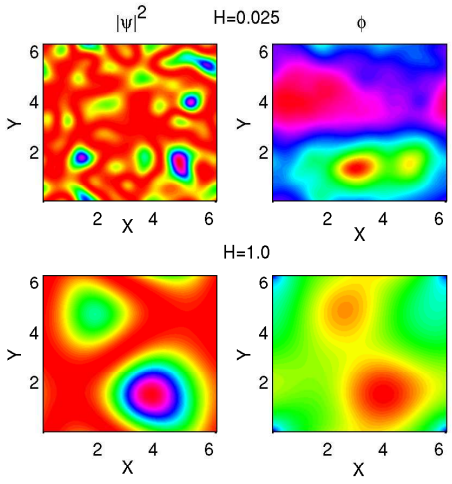

FIG. 1: Small scale fluctuations in the electron density resulted from a steady turbulence simulations of our 2D electron plasma. Forward cascades are responsible for the generation of small-scale fluctuations (top left). (Top right) Large scale structures are present in the electrostatic potential, essentially resulting from an inverse cascade. The parameter H is 0.025 and 1.0 respectilvely for the upper and lower panels. Lower panel shows predominance of large scale structures in both electron density (left) and ES potential (right).

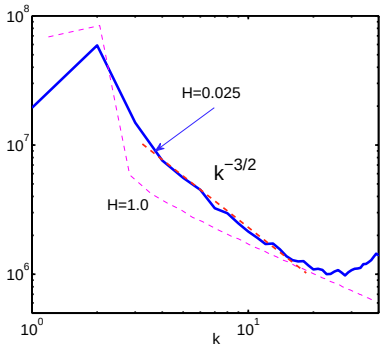

FIG. 2: The 2D electron fluid turbulence interestingly relaxes towards an Iroshnikov-Kraichnan (IK) type $k^{-3/2}$ spectrum in a dense plasma. Here $H = 0.025$ for the solid curve. The dotted curve corresponding to $H = 1.0$ exhibits a condensation phenomenon in which both the electron density and potential are dominated by the large scales, whereas the spectrum shows a sharp rise in the lower band. This is further consistent with Fig 1 (lower panel).

right). It is to be noted that the co-existence of the small and larger scale structures in turbulence is a ubiquitous feature of various 2D turbulence systems. For example, in 2D hydrodynamic turbulence, the incompressible fluid admits two invariants, namely the energy and the mean squared vorticity. The two invariants, under the action of an external forcing, cascade simultaneously in turbulence, thereby leading to a dual cascade phenomena. In these processes, the energy cascades towards longer length-scales, while the fluid vorticity transfers spectral power towards shorter length-scales. Usually, a dual cascade is observed in a driven turbulence simulation, in which certain modes are excited externally through random turbulent forces in spectral space. The randomly excited Fourier modes transfer the spectral energy by conserving the constants of motion in k-space. On the other hand, in freely decaying turbulence, the energy contained in the large-scale eddies is transferred to the smaller scales, leading to a statistically stationary inertial regime associated with the forward cascades of one of the invariants. Decaying turbulence often leads to the formation of coherent structures as turbulence relaxes, thus making the nonlinear interactions rather inefficient when they are saturated. The power spectrum exhibits an interesting feature in our 2D electron plasma system, unlike the 2D hydrodynamic turbulence [19, 20]. The spectral slope in the 2D quantum electron fluid turbulence is close to the Iroshnikov-Kraichnan power law [21, 22] $k^{-3/2}$, rather than the usual Kolomogrov power law [19] $k^{-5/3}$. This is shown in Fig 2 (solid curve). Physically, the deviation from the $k^{-5/3}$ exponent comes about because the short wavelength part of the EPOs spectrum is controlled by the quantum tunneling effect associated with the Bohm potential. The peak in the energy spectrum can be attributed to the higher turbulent power residing in the EPO potential, which eventually leads to the generation of larger scale structures, as the total energy encompasses both the electrostatic potential and electron density components. In our dual cascade process, there is a delicate competition between the EPO dispersions caused by the statistical pressure law (giving the $k^2V_F^2$ term, which dominates at longer scales) and the quantum Bohm potential (giving the $\hbar^2k^4/4m_e^2$ term, which dominates at shorter scales with respect to a source). Furthermore, it is interesting to note that exponents other than $k^{-5/3}$ have also been observed in numerical simulations [23] of the Charney and 2D incompressible Navier-Stokes equations. The dual cascades, shown in Fig 1 (top panel), can further be contrasted with $H > 1$ case. The latter modifies the characteristic of turbulence by condensating the energy in the lower Fourier modes. Hence the spectra of electron density and potential are dominated by the large scales as shown in Fig 1 (bottom panel). The turbulent spectrum is therefore peaked essentially at the lower band as illustrated by the dotted curve in Fig 2 ($H = 1$ curve).

We finally estimate the electron diffusion coefficient in the presence of small and large scale turbulent EPOs in our quantum plasma. An effective electron diffusion coefficient caused by the momentum transfer can be calculated from $D_{eff} = \int_0^\infty \langle \mathbf{P}(\mathbf{r},t)\cdot\mathbf{P}(\mathbf{r},t+t')\rangle dt'$, where the angular bracket denotes spatial averages and the ensemble averages are normalized to unit mass. Since the 2D structures are confined to a $x-y$ plane, the effective electron diffusion coefficient, D_{eff}, essentially relates the diffusion processes associated with random translational motions of the electrons in nonlinear plasmonic fields. We

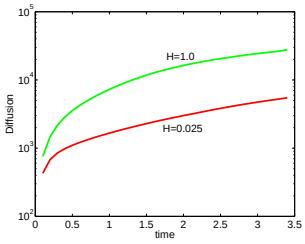

FIG. 3: Time evolution of an effective electron diffusion coefficient. Upper curve corresponds to the diffusion associated with the large-scale structures for $H = 1.0$, whereas the lower curve represents a diffusion corresponding to the $H = 0.025$. The former is consistent with the Fig 1 (lower panel) and Fig 2 (dotted curve).

compute D_{eff} in our simulations, to measure the turbulent electron transport that is associated with the turbulent structures that we have reported herein. It is observed that the effective electron diffusion is lower when the field perturbations are Gaussian. On the other hand, the electron diffusion increases rapidly with the eventual formation of longer length-scale structures, as shown in Fig. 3. The electron diffusion mediated by the large scale structures in quantum plasmas dominates substantially in the presence of condensation effects i.e. $H = 1$, as elucidated in Fig. 3 (top curve). Furthermore, in the steady-state, nonlinearly coupled EPOs form stationary structures, and D_{eff} saturates eventually. Thus, remarkably an enhanced electron diffusion results primarily due to the emergence of large-scale potential structures in our 2D quantum plasma.

In summary, we have presented computer simulation studies of the 2D fluid turbulence in a dense quantum plasma. Our simulations, for the parameters that are representative of the next generation intense laser-solid density plasma experiments as well as of the superdense astrophysical bodies, reveal new features of the dual cascade in a fully developed 2D electron fluid turbulence. Specifically, we find that the power spectrum associated with nonlinearly interacting EPOs in (weak) quantum plasmas follow a non-Kolmogorov-like spectrum. The deviation from a Kolmogorov-like spectrum resulting from the flattening of the spectrum is mediated essentially by the nonlinear EPOs interactions in the inertial range (basically controlled by the electron plasma wave dispersion effect represented by $\hbar^2 k^4/4m_e^2$), which impedes the spectral transfer of the turbulent power associated with the short scale Fourier modes. In the nonlinear regime, the inhibition of the spectral transfer is caused by short scale EPOs that are nonlinearly excited by the mode coupling of the EPOs in the forward cascade regime, which then grow, acquire nonlinear amplitudes, and eventually saturate in the nonlinear phase.

[1] D. Pines, J. Nucl. Energy: Part C: Plasma Phys. **2**, 5 (1961).
[2] C. L. Gardner and C. Ringhofer, Phys. Rev. E **53**, 157 (1996).
[3] L. K. Ang *et al.*, Phys. Rev. Lett. **91**, 208303 (2003); L. K. Ang and P. Zhang, *ibid.* **98**, 164802 (2007).
[4] G. Manfredi and F. Haas, Phys. Rev. B **64**, 075316 (2001).
[5] G. Manfredi, Fields Inst. Commun. **46**, 263 (2005).
[6] F. Haas, Phys. Plasmas **12**, 062117 (2005).
[7] P. K. Shukla and B. Eliasson, Phys. Rev. Lett. **96**, 245001 (2006).
[8] P. Hohenberg and W. Kohn, Phys. Rev. **136**, B864 (1964); W. Kohn and L. J. Sham, Phys. Rev. **140**, A1133 (1965); L. Brey *et al.*, Phys. Rev. B **42**, 1240 (1990).
[9] M. Marklund and G. Brodin, Phys. Rev. Lett. **98**, 025001 (2007).
[10] G. Mourou *et al.*, Rev. Mod. Phys. **78**, 309 (2006); Y. A. Salamin *et al.*, Phys. Rep. **427**, 41 (2006).
[11] V. M. Malkin *et al.*, Phys. Rev. E **75**, 026404 (2007).
[12] G. Chabrier *et al.*, J. Phys.: Condens. Matter **14**, 9133 (2002); J. Phys. A: Math. Gen. **39**, 4411 (2006).
[13] A. K. Harding and D. Lai, Rep. Prog. Phys. **69**, 2631 (2006).
[14] G. V. Shpatakovskaya, J. Exp. Teor. Phys. **102**, 466 (2006).
[15] W. L. Barnes *et al.*, Nature (London) **424**, 824 (2003); D. E. Chang *et al.*, Phys. Rev. Lett. **97**, 053002 (2006).
[16] E. P. Wigner, Phys. Rev. **40**, 749 (1932); M. Hillery *et al.*, Phys. Rep. **106**, 121 (1984).
[17] D. Gottlieb and S. A. Orszag, Numerical Analysis of Spectral Methods, SIAM, Philadelphia, 1977
[18] I. Iben Jr. and A. V. Tutukov, Astrophys. J. **282**, 615 (1984).
[19] A. N. Kolmogorov, C.R. Acad. Sci. USSR **30**, 301 (1941).
[20] M. Lesieur, *Turbulence in Fluids* (Kluwer, Dordrecht, 1990); U. Frisch, *Turbulence* (Cambridge University Press, Cambridge, England, 1995).
[21] P. Iroshnikov, Sov. Astron. **7**, 566 (1963).
[22] R. H. Kraichnan, Phys. Fluids **8**, 1385 (1965).
[23] V. D. Larichev and J. C. McWilliams, Phys. Fluids A **3** 938 (1991); R. K. Scott, Phys. Rev. E **75**, 046301 (2007).

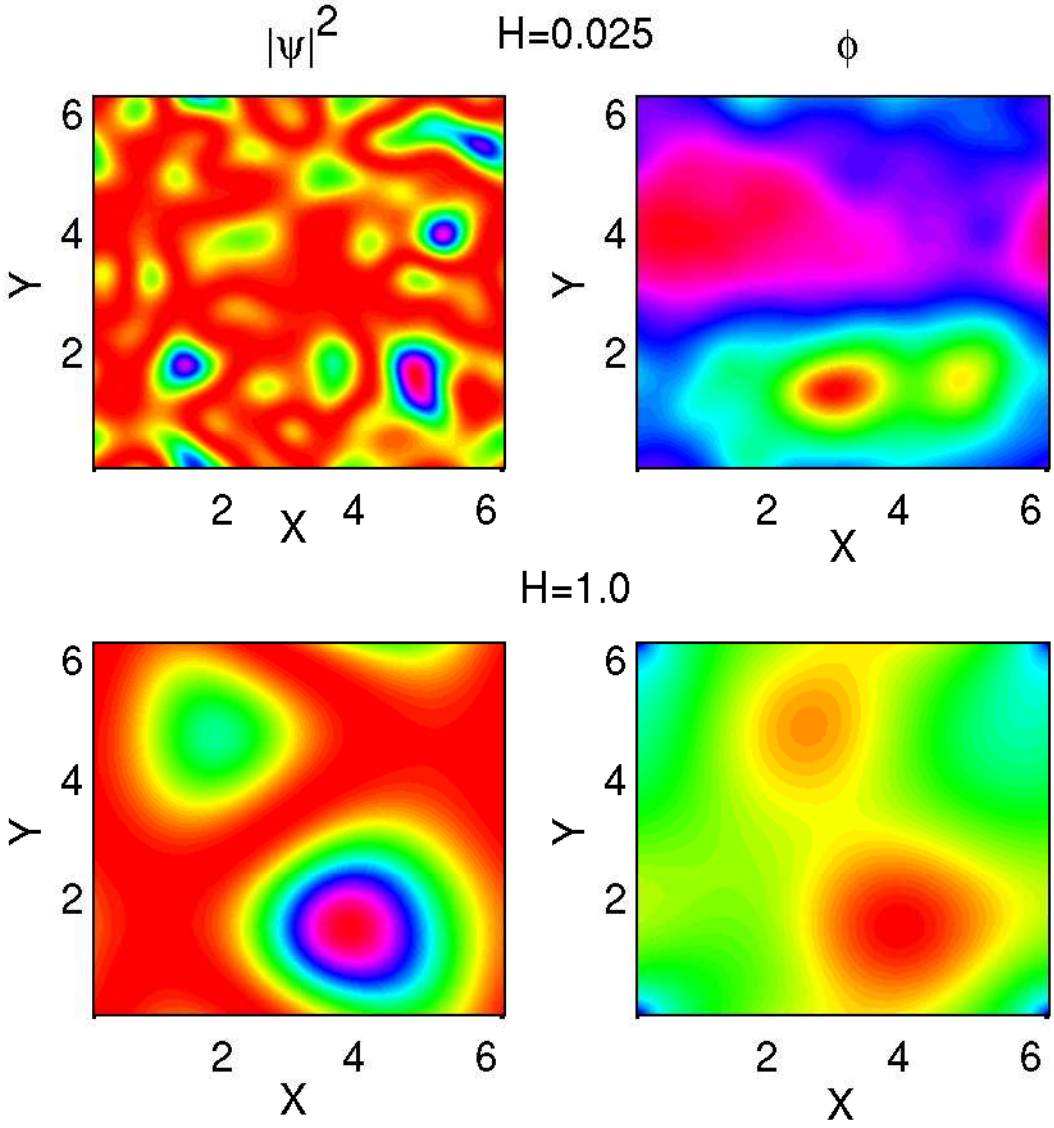

Figure 1

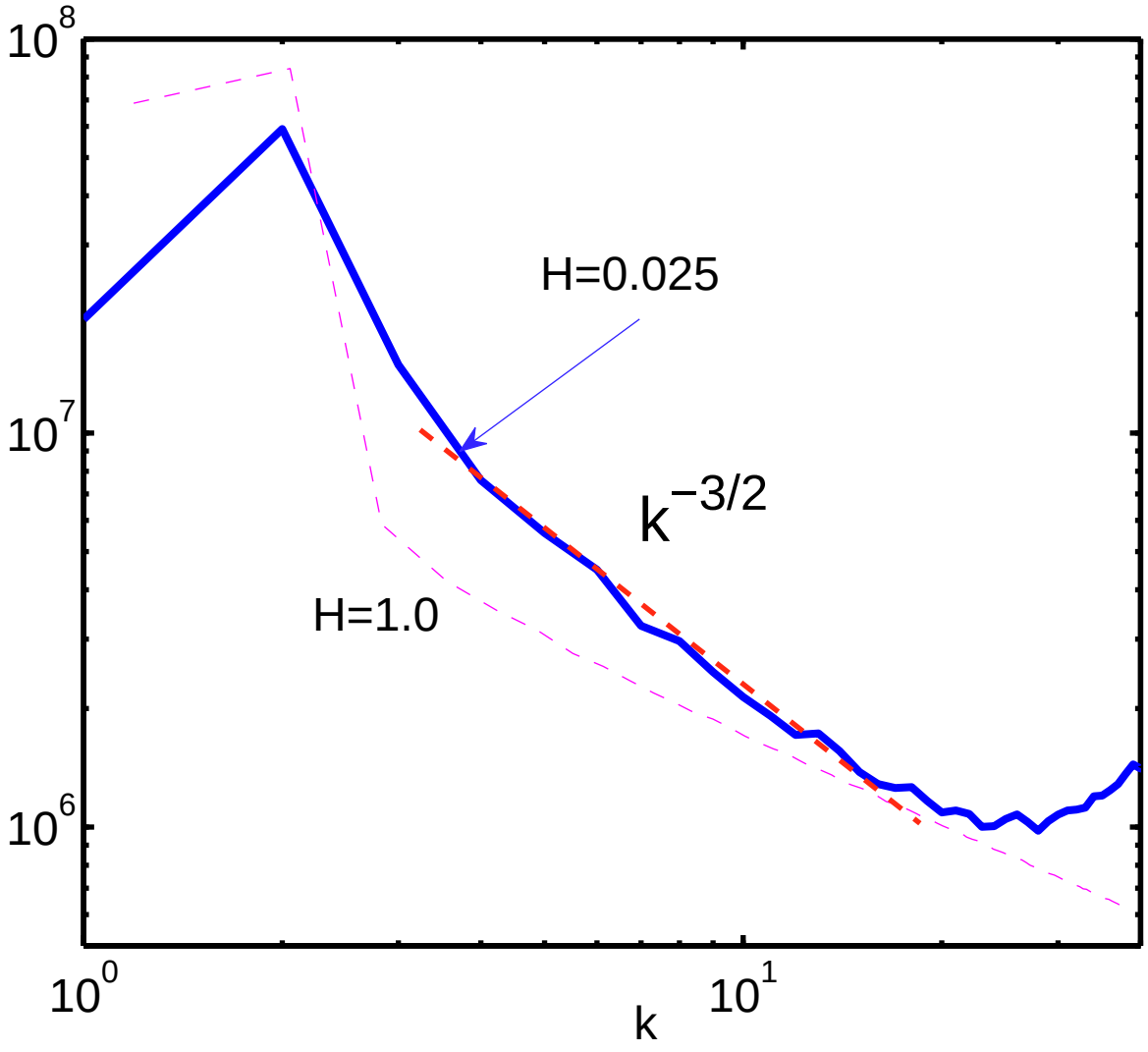

Figure 2

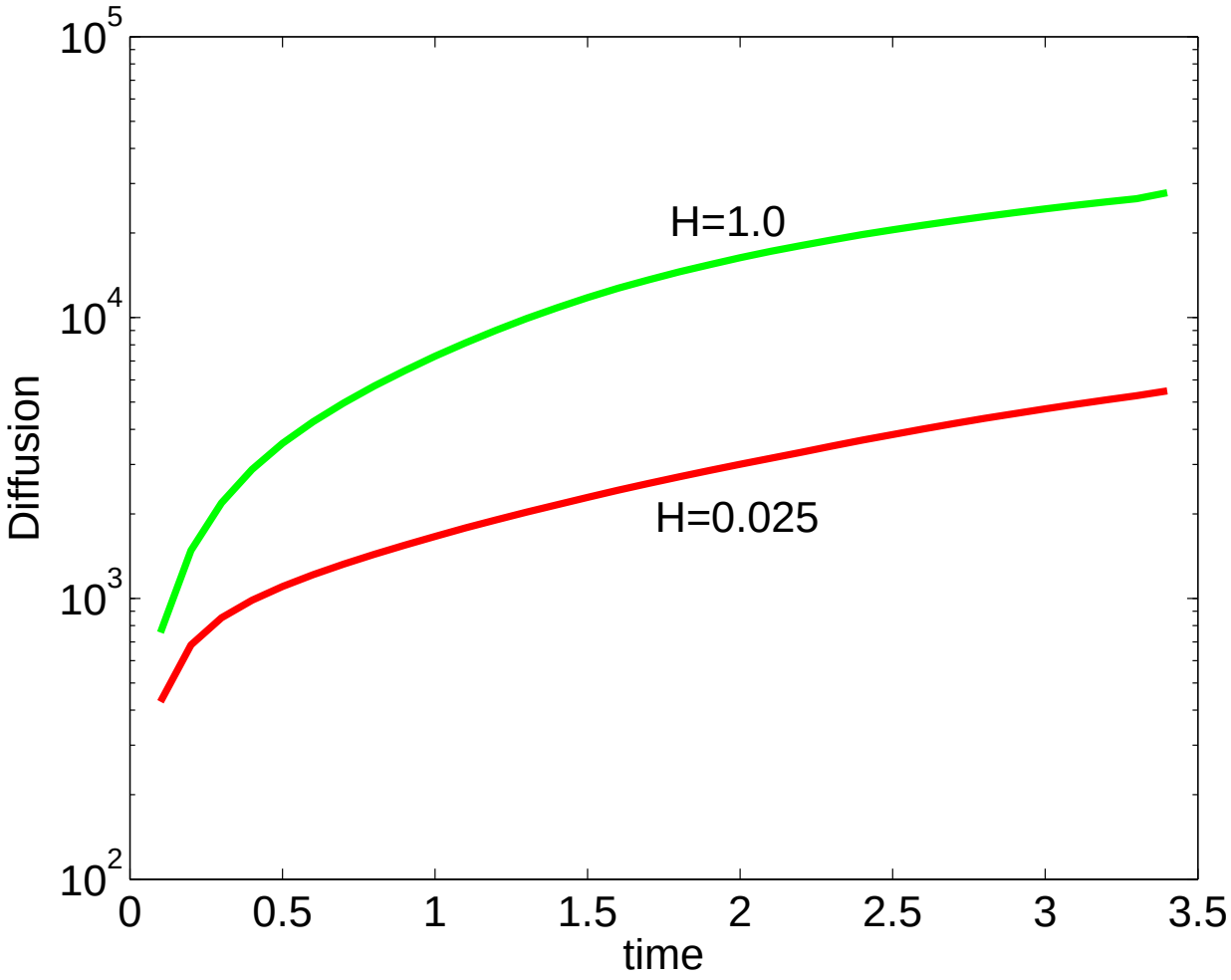

Figure 3